Atmos. Chem. Phys. Discuss., 3, 1247–1272, 2003
www.atmos-chem-phys.org/acpd/3/1247/

Atmospheric Chemistry and Physics Discussions

Distribution and origin of ozone in the eastern Mediterranean free troposphere during MINOS (August 2001)

G.-J. Roelofs[1], B. Scheeren[1, 3], J. Heland[2], H. Ziereis[2], and J. Lelieveld[3]

[1]Institute for Marine and Atmospheric Research, Utrecht University, 3508 TA Utrecht, The Netherlands
[2]Institute for Atmospheric Physics, Deutsches Zentrum für Luft- und Raumfahrt, Oberpfaffenhofen, Germany
[3]Max Planck Institute for Chemistry, Mainz, Germany

Received: 12 December 2002 – Accepted: 13 February 2003 – Published: 5 March 2003

Correspondence to: G.-J. Roelofs (g.j.roelofs@phys.uu.nl)

Abstract

A coupled tropospheric chemistry – climate model is used to reproduce and analyze tropospheric ozone distributions observed during the MINOS campaign in the eastern Mediterranean region (August, 2001). Generally, regional atmospheric dynamics in summer are strongly influenced by the occurrence of an upper tropospheric anti-cyclone, associated with the Asian summer monsoon and centered over the Tibetan Plateau. The anti-cyclone affects the chemical composition of the upper troposphere, where ozone concentrations of about 50 ppbv were measured, through advection of boundary layer air from South-East Asia. A layer between 4–6 km thickness and containing up to 120 ppbv of ozone was present beneath. Ozone from stratospheric origin and from lightning NO_x contributed to this layer. Additionally, pollutant ozone from North America was mixed in. Ozone in the lower troposphere originated mainly from the European continent. Modeled ozone profiles are in reasonable agreement with the observations. The stratospheric influence is sometimes overestimated by the model due to too strong vertical diffusion associated with the relatively coarse vertical resolution of the model, and specific convective events are not reproduced realistically. The modeled tropospheric ozone column over the eastern Mediterranean is ~50 DU in summer, to which ozone from recent stratospheric origin contributes about 30%, ozone from lightning 13%, and from South-East Asia, North America and Europe about 7%, 8% and 14%, respectively, adding to a long-term hemispheric background of 25% of the column.

1. Introduction

The MINOS measurement campaign (Mediterranean INtensive Oxidant Study) was conducted from Crete in the eastern Mediterranean region during July/August 2001. Earlier measurements and model studies indicate that the combination of pollution transports into the region and cloud-free conditions enable efficient photochemical ac-

ACPD

3, 1247–1272, 2003

tivity producing relatively high concentrations of, e.g. ozone and oxidized organics (Kouvarakis et al., 2000). The objective of MINOS was to observe and understand the chemical composition of tropospheric air in the Mediterranean region in terms of atmospheric transport and chemistry. MINOS employed a ground-based and an aircraft-based measurement platform to observe atmospheric ozone, CO, higher hydrocarbons, nitrogen oxides and aerosols. An overview of the MINOS results is presented in Lelieveld et al. (2002) while other aspects of the MINOS campaign are presented in this issue.

This model study focuses on the distribution of ozone in the Mediterranean region during MINOS, with an emphasis on the free troposphere. We simulated the photochemistry and transports for the summer of 2001 with a coupled tropospheric chemistry-climate model. The model is described in Sect. 2. In Sect. 3 we evaluate the model performance by comparing measured and modeled ozone profiles, and we analyze governing transports by means of backward trajectory calculations. In Sect. 4 we present the simulated ozone distribution over the eastern Mediterranean region and briefly discuss the governing atmospheric dynamics affecting the region. In Sect. 5 the modeled ozone distribution is analyzed in terms of contributions from the major ozone precursor source regions. Conclusions are presented in Sect. 6.

2. Model description

The general circulation model (GCM) used in this study is the European Centre Hamburg model version 4 (ECHAM4), with a horizontal resolution of $1.8^{\circ} \times 1.8^{\circ}$ and a time step of 900 s (T63). The model distinguishes 19 hybrid σ-p layers between the surface and the top level at 10 hPa. Average pressure levels relevant for the troposphere and lower stratosphere are 995, 980, 950, 908, 846, 770, 680, 590, 495, 405, 320, 250, 190, 140, 100 and 73 hPa referring to approximate altitudes of 0.03, 0.14, 0.38, 0.77, 1.4, 2.1, 3.1, 4.2, 5.4, 6.8, 8.3, 10, 12, 13.8, 15.7 and 18 km above the surface. Tracer transport is calculated with a semi-Langrangian advection scheme (Rasch and

Williamson, 1990). Additional vertical transports are included through the parameterisation of vertical diffusion and convection. Detailed information on ECHAM is given by Roeckner et al. (1996). We developed a tropospheric chemistry scheme describing emissions of NO, CO and non-methane hydrocarbons (NMHC), dry deposition of O_3, NO_2, HNO_3 and H_2O_2, wet deposition of HNO_3 and H_2O_2, while the CBM4 scheme represents higher hydrocarbon chemistry. This has been coupled to ECHAM (Roelofs and Lelieveld, 1995, 2000a; Ganzeveld et al., 1998).

Because the model does not represent typical stratospheric chemistry, ozone in the stratosphere is parameterised with results from a 2D troposphere-stratosphere chemistry model (Brühl and Crutzen, 1988). Additionally, the model applies an ozone-potential vorticity (PV) correlation in the extra-tropical lower stratosphere (LS) to preserve longitudinal variability of ozone associated with the meandering and breaking of the jet streams (Roelofs and Lelieveld, 2000b). The parameterisation is applied above the extra-tropical tropopause while transport and mixing in the tropopause region is simulated by the model.

The model considers a separate stratospheric ozone tracer, referred to as O_3s. The concentration of O_3s is equal to that of ozone in the grids where stratospheric ozone is prescribed. O_3s is transported from the stratosphere into the troposphere along with the calculated air motions, where it is photochemically destroyed or removed by dry deposition. The difference between O_3 and O_3s is a measure of ozone that originates from photochemical production, mainly in the troposphere, and is referred to as O_3t. Applications and further discussion of the method are presented in Roelofs and Lelieveld (2000a) and Kentarchos and Roelofs (2003).

The simulated ozone seasonalities at the surface, in the free troposphere and in the tropopause region agree well with observations (e.g. Roelofs and Lelieveld, 2000a). The same is true for ozone distributions during specific meteorological conditions, e.g. synoptic disturbances (Roelofs and Lelieveld, 2000b; Kentarchos et al., 2001), although the model may overestimate the downward transport efficiency of stratospheric ozone into the troposphere because of the relatively coarse vertical resolution near the

tropopause and the rather diffusive semi-Lagrangian transport scheme (Meloen et al., 2003; Roelofs et al., 2003).

In this study we use the model in a "nudged" mode, i.e. the model is forced to simulate specific meteorological conditions in July and August 2001, by assimilating ECMWF analyzed distributions of surface pressure, temperature, vorticity and divergence (Jeuken et al., 1996). We note that the model considers climatological emission data for ozone precursors (see Roelofs and Lelieveld, 2000a), which may not be consistent with the actual emissions during the MINOS period, in particular from unpredictable sources such as biomass burning.

3. Comparison of observed and simulated ozone

MINOS encompassed fourteen measurement flights with the Falcon aircraft of the DLR (Deutsches Zentrum für Luft- und Raumfahrt, Germany), conducted from the airport of Heraklion (Crete, 35° N, 25° E). Ozone was measured by UV absorption with a modified TE (Thermo Environmental) 49 instrument with an accuracy of 5%. Detailed information about the measurement flights and data can be found in Heland et al. (2003). In this section we compare the modeled ozone profiles with those observed for four measurement flights, and analyze the profiles in terms of the actual dynamical and meteorological conditions. Figure 1 shows observed ozone concentrations with a time resolution of 12 s, for the flights on 8, 14, 16 and 22 August. Modeled concentrations are given by the red (total ozone), blue (O_3s) and green (O_3t) lines. The flights represent different meteorological and atmospheric chemical conditions and illustrate the associated model representativity.

3.1. 8 August, flight 03

During flight 03 the aircraft traveled eastwards to approximately 28°E, where it made a north-south transect of approximately 2°. The aircraft was between 10 and 14 km

altitude during most of the 3-h flight, with an ascent and descent of approximately 30 min each. The results show very good agreement between modeled and observed ozone concentrations in the free troposphere (Fig. 1a) and vertical ozone gradients are captured well.

Figure 2 presents 8-day backward trajectories from different altitudes in the free troposphere. These have been computed with a trajectory model made available by the British Atmospheric Data Center that uses ECMWF analyzed horizontal and vertical winds (u, v, ω) on a horizontal resolution of 2.5° × 2.5° (http://www.badctraj.rl.ac.uk/). The trajectories ending above 300 hPa originate from SE Asia. The analysis presented by Scheeren et al. (2003) demonstrates that associated trace gases originate from the boundary layer in India, and are transported upward by convection into an upper tropospheric anti-cyclone centered over the Tibetan plateau. This anti-cyclone is a typical large-scale feature in the summer, extending over southern Asia and northwest Africa, and influenced by the Asian summer monsoon (ASM) (Barry and Chorly, 1987).

Mid-tropospheric air (400-600 hPa), on the other hand, was advected from the west, being characterized by relatively high ozone levels. This air descended from the upper troposphere (UT) and the tropopause region only a few days earlier, after residing in the tropopause region for at least the 5 preceding days. Simulated O_3s suggests an important influence from the stratosphere, and the high ozone content may be explained by a preceding STE event. The C-shape of the observed CO profile with ~70 ppbv CO between 4 and 8 km altitude, and ~100 ppbv CO in the UT (Lawrence et al., 2002), supports this explanation. We note that CO distributions are generally reproduced well by our model (Roelofs and Lelieveld, 2000a), which was also the case for MINOS.

Backward trajectories ending in the boundary layer and the lower troposphere lead across Eastern Europe, mainly Russia and the Ukraine. The model simulates a realistic ozone concentration gradient between the boundary layer and the free troposphere, although absolute concentrations are overestimated. We will not elaborately discuss boundary layer chemistry and transports. The horizontal and vertical resolutions of the model are too coarse to accurately represent some of the relevant boundary layer

characteristics in detail, e.g. height and stability or the occurrence of land-sea breeze circulations, while accurate emission estimates, e.g. for biomass burning in eastern Europe, which have a significant impact on the Mediterranean boundary layer (Traub et al., 2003), are not available yet. The generally good agreement between model and measurements supports the result that O3t contributes 40–50 ppbv ozone throughout the free troposphere. This will be further analyzed in the next section.

3.2. 14 August, flight 06

On flight 06 on 14 August the aircraft flew approximately 2° northward from Crete and back. Both parts of the 4-h flight consisted of a swift ascent to about 10 km altitude and a descent in intervals to the boundary layer. Ozone concentrations between 40 and 70 ppbv were observed, with peaks up to 100 ppbv between 2 and 3 km and between 8 and 9 km altitude (see Fig. 1b). The latter peak can be explained by the vicinity of the tropopause and the lower stratosphere. It is captured by the model, but ozone levels are underestimated, probably due to the relatively coarse vertical resolution around the tropopause (~1.5 km) resulting in an underestimate of the steep ozone concentration gradient in the UTLS. The observed ozone maximum at 2–3 km altitude is not fully reproduced by the model. Observed concentrations of organic trace species in this air mass also significantly exceed background values (J. de Gouw, personal communication), precluding a stratospheric origin.

The simulated O_3s profile maximizes between 3 and 5 km altitude while the O_3t profile has a minimum. According to the backward trajectory analysis shown in Fig. 3, the sampled air originates partly from the UT where ozone-rich conditions prevail, and partly from the sub-tropical Atlantic middle and low troposphere (3–7 km) where ozone concentrations are relatively low. The latter trajectory is consistent with a 15-year climatological study of STE with a Lagrangian model in which the sub-tropical western North-Atlantic area is shown to be a region with relatively strong transport of lower tropospheric air into the UTLS (Sprenger and Wernli, 2003). The transport routes originating from the upper and from the lower troposphere are part of synoptic disturbances

travelling across the Atlantic Ocean to Europe, following the wave-like path shown in Fig. 3. Modeled ozone concentrations between 4 and 8 km altitude are at the high end of the observed range for this flight, probably due to the relatively diffusive semi-Lagrangian transport scheme applied in our model and the coarse vertical resolution around the tropopause as mentioned above.

3.3. 16 August, flight 08

During flight 08 on 16 August the aircraft flew in north-westerly direction to approximately 38° N, 20° E. Most of the 3-h flight was upper tropospheric, but contrary to flight 03 the sampled air contained relatively much ozone (Fig. 1c). The simulated O_3s suggests a stratospheric origin for this. The model simulates higher ozone levels at 12-14 km altitude, close to the tropopause, although lower than observed. The magnitude of the ozone peak at 10–11 km altitude, also characterized by a large contribution from the stratosphere, is captured more realistically by the model.

Ozone in the mid-troposphere is overestimated by 10–15 ppbv, which may again be due to the overestimation of downward cross-tropopause ozone transports. A lower tropospheric ozone maximum is observed at 2–3 km altitude, but not modeled. Such peaks above the boundary layer are typical for the influence by shallow convection, e.g. in land-sea breezes and orographic flows that carry pollutants into a reservoir layer (Millan et al., 1997). This is not reproduced realistically by the model. Relatively high concentrations of organic trace species are also observed in this air mass, up to ~3 ppb acetone, ~5 ppb methanol, and 700 ppt acetaldehyde (J. de Gouw, personal communication; see also De Gouw et al., 2003). Backward trajectories (not shown) indicate that the air was advected from the west across southern France, northern Italy and Greece while remaining between 600 and 750 hPa (2-4 km altitude) in the 5 previous days.

ACPD
3, 1247–1272, 2003

3.4. 22 August, flight 14

On flight 14 on 22 August the aircraft flew from Sardinia (8.6° E, 40.5° N) to Crete. The altitude during the 3-h flight was partly 9 km and mostly 12 km. In contrast with the flights presented thus far, a more gradual ozone increase with height was measured on this flight (Fig. 1d). The model results indicate that this ozone increase is associated with stratospheric influence, while the contribution from photochemical production in the troposphere decreases with altitude. In the next section it is shown that the UT ASM anti-cyclone briefly retreated eastward from the region during this period. Although the vertical profile is simulated realistically, peak ozone concentrations between 9 km (>100 ppbv) and 12 km altitude (>150 ppbv) are not reproduced by the model. Similar to the previous flight this is probably due to the relatively coarse vertical resolution near the tropopause.

4. Simulated ozone distribution

Figure 4 shows time-altitude plots of simulated ozone between 19 July and 30 August 2001 (days 200–240) above Crete. Also shown are the contributions from ozone from stratospheric origin (O_3s) and from photochemical formation in the troposphere (O_3t). For reference we note that the MINOS flights 3, 6, 8 and 14 which are discussed in the previous section correspond with days 220, 226, 228 and 234.

The UT, between approximately 9 and 16 km, is characterized by ozone levels between 45 and 55 ppbv, while ozone levels in the lower troposphere are generally between 70 and 90 ppbv. Relatively high ozone concentrations are simulated between 3 and 9 km altitude almost throughout the 40 days considered here. As discussed in the previous section, the simulated mid-tropospheric ozone maximum is associated with ozone of stratospheric origin (Fig. 4b). The calculated contribution of O_3s to tropospheric ozone in this layer generally exceeds 30% and sometimes even 60%, directly associated with synoptic systems that travel from the North-Atlantic to Europe, while

ACPD
3, 1247–1272, 2003

O_3s contributions below 10% are simulated above and below this layer. The typical summer conditions in the eastern Mediterranean atmosphere are illustrated in Fig. 5, which shows a latitude-height distribution of the potential temperature along 25° E for 3 August (day 216). Below the UT, where the ASM anti-cyclone occurs, a more stable layer exists with a relatively steep potential temperature gradient, between −9° and −6° km^{-1}. This forms a channel between the lower stratosphere at high latitudes and the middle troposphere at lower latitudes. Enclosed between two less stable air masses (i.e. the ASM anti-cyclone and the lower troposphere) and almost parallel to the isentropes, this layer acts as a funnel through which extra-tropical UTLS air is efficiently transported south-, east- and downward. This is illustrated by the potential vorticity distribution (PV; 1 PV unit = 10^{-6} km^2 kg^{-1} s^{-1}) also displayed in Fig. 5, which shows a characteristic high-PV tongue of air in the stable layer. The tropopause height, defined as the 2 PVU level, is approximately 15–16 km altitude above Crete. The situation described here is briefly interrupted between days 232 and 236 when the UT anti-cyclone retreated eastward for a few days. This resulted in a lower tropopause height over the eastern Mediterranean region and, hence, higher ozone levels, 80–100 ppbv, in the UT. Ozone from in-situ photochemical formation (O_3t) is 40–60 ppbv in the free troposphere (Fig. 4c). In addition to the stratospheric contribution discussed above, other ozone or ozone precursor source regions are found to significantly contribute to the tropospheric ozone column over the eastern Mediterranean. This is analyzed further in the next section.

5. Regional contributions to tropospheric ozone during MINOS

We performed a series of sensitivity runs in which anthropogenic and natural emissions of NO_x, CO and NMHC were omitted for the regions listed in Table 1. In another simulation NO_x emissions from lightning, which may contribute significantly to tropospheric ozone (Lelieveld and Dentener, 2000), were omitted. A specific contribution is calculated as the difference between the control simulation, i.e. with all emissions

ACPD
3, 1247–1272, 2003

considered, and a sensitivity run. All simulations started on 1 January 2001, allowing a mixing throughout the NH of the chemical effects due to the emission changes.

It must be noted that the decrease of the ozone production due to the ozone precursor emission reductions in the sensitivity simulations may be partly offset by an increase of the ozone production efficiency per NO_x molecule. Changes in the calculated photodissociation rates, for which the model ozone serves as input, may have an additional effect. Additionally, we performed a simulation that only considered the ozone precursor emissions from the regions listed in Table 1, from lightning and the ozone source from the stratosphere. The difference between this and the control simulation represents the amount of O_3t that can not be assigned to the source regions considered, and which we will refer to as "background residual". To minimize the effect of the chemical compensation effects the regional and residual contributions where scaled so that their sum equals O_3t from the control simulation. The scaling factor varies between about 1.10 in the UT to 1.25 in the boundary layer.

Figure 6 shows the calculated contributions to ozone from each of the regions and from lightning. Again the tropospheric layering over the eastern Mediterranean region is illustrated, with the SE Asian contribution in the UT, the North American and, albeit relatively small, African contribution in the middle troposphere, and the western and eastern European contributions in the lower troposphere.

The ozone precursor emissions from India and China together contribute up to 25 ppbv of ozone in the UT. This contributes 30–50% to O_3t. Around 22 August (day 234) the SE Asian contribution diminishes for a few days due to a weakening of the anti-cyclonic influence in the region.

The main contributions to ozone in the mid-troposphere, apart from O_3s discussed in Sect. 4, are from North America and from lightning. The North American contribution ranges between 6 and 12 ppbv. The maximum in North American ozone between days 219 and 222 is associated with a synoptic disturbance that also causes a peak in O_3s on day 220 (Fig. 4b). The role of synoptic disturbances as a mechanism for cross-Atlantic transport of North American pollution has been discussed by Stohl and

ACPD
3, 1247–1272, 2003

Trickl (1999), and our model results indicate that similar transports occurred during MINOS. Note that when the ASM anti-cyclone retreats, between days 231 and 236, the North American contribution extends throughout the depth of the troposphere, which increases its contribution to the tropospheric ozone column by ∼50%. It appears that the presence of the ASM anti-cyclone over the eastern Mediterranean limits the vertical dispersion of North American pollution in the free troposphere, thereby suppressing associated ozone production.

Ozone from lightning NO_x also maximizes in the mid-troposphere, possibly associated with convection in synoptic systems. It contributes up to 35% of O_3t at this altitude. At altitudes dominated by the ASM anti-cyclone the contribution by lightning is also relatively large, 6–10 ppbv ozone or 15–25% of the O_3t. Here, lightning ozone is probably associated with the monsoon convection south of the Tibetan plateau, which also transports SE Asian boundary layer air into the UT anti-cyclone. Finally, ozone precursor emissions from Africa have a relatively small influence, 2–4 ppbv, on ozone in the mid-troposphere.

The effect of eastern European precursor emissions is limited to altitudes below 3 km, with contributions up to 55 ppbv at the surface. Ozone concentrations from western European precursor emissions are smaller but their contribution extends further upward, up to 5 km altitude. The results clearly illustrate that the stable mid-tropospheric layer suppresses mixing between the boundary layer and the free troposphere so that European pollution does not significantly affect free tropospheric ozone. However, it is possible that shallow convection plays a role. On days 226–227 a small maximum of western European ozone occurs at 3 km altitude. This probably corresponds with the lower tropospheric ozone maximum measured on flight 08 and discussed in Sect. 3. As mentioned above, the small-scale plumes are not resolved adequately by the model.

The background residual ozone fraction in the free troposphere amounts to 15–20 ppbv. It originates from all other natural and anthropogenic precursor emissions in the northern hemisphere. In the boundary layer the residual exceeds 30 ppbv on days 206 and 214, associated with easterly transport of pollution from the Istanbul

ACPD
3, 1247–1272, 2003

area (Turkey) (see also Traub et al., 2003). In the free troposphere, the residual is larger than the direct contribution by any of the source regions except the stratosphere.

The regional contributions are summarized in Table 2 which lists the computed tropospheric ozone column above Crete, averaged between days 200 and 225, i.e. with the UT anti-cyclone present, and integrated between the surface and the model tropopause at 15–16 km altitude. The computed tropospheric ozone column above Crete is nearly 50 DU (Dobson Unit; 1 DU = 2.69×10^{16} molecules $O_3\,cm^{-2}$). This is, for example, comparable with the ozone column maximum of 50–60 DU over the tropical southern Atlantic Ocean in austral spring, under influence of strong biomass burning emissions (e.g. Thompson et al., 1996). Our study indicates that the tropospheric ozone column over the eastern Mediterranean contains a substantial contribution by natural sources, with about 40% originating from the stratospheric and lightning sources together, although the calculated contribution by stratospheric ozone is probably an upper limit.

6. Conclusions

We investigated the distribution and sources of free tropospheric ozone over the Mediterranean area in July and August 2001 with a coupled tropospheric chemistry-GCM. Model results were compared with aircraft measurements of ozone from the MINOS field campaign.

The model simulates three distinct ozone layers in the troposphere over the eastern Mediterranean region for the summer of 2001. The uppermost layer, between 9 km altitude and the tropopause at 15–16 km, is strongly influenced by the western branch of a large UT anti-cyclone centered over the Tibetan plateau associated with the Asian monsoon. Air pollution originating from the South and SE Asian boundary layer can thus reach the Mediterranean UT. The model simulates 40-55 ppbv ozone in this region, of which up to 20 ppbv derives from natural and anthropogenic emissions in South and SE Asia.

The anti-cyclone influences potential temperature and vorticity distributions in the

UT in the region so that a relatively stable layer is created in the mid-troposphere along which relatively ozone-rich air from higher latitudes is efficiently transported downward and southeastward. In the Mediterranean region this appears as a layer with 65–100 ppbv ozone at 3 to 8 km altitude between the UT anti-cyclone and the boundary layer. Between 25 and 60 ppbv of ozone in this layer derives from the stratosphere. At several instances during MINOS cross-Atlantic transport of North American air adds to this mid-tropospheric ozone layer, with the largest contribution of 8–10 ppbv coinciding with the passage of synoptic disturbances around 7 August. Lightning is an additional important source of ozone to this layer, contributing 10–20 ppbv.

Lower tropospheric ozone over the eastern Mediterranean region is strongly influenced by precursor emissions from eastern Europe, remaining in the boundary layer, and from western Europe in and directly above the boundary layer. Upward mixing into the free troposphere is efficiently suppressed by the stable layer aloft. The typical layering in the region was briefly interrupted around 20 August when the influence of the UT anti-cyclone on the atmospheric layering decreased, with more vigorous mixing of pollutants throughout the depth of the troposphere as a result.

Comparison of modeled and observed ozone profiles generally shows good agreement, indicating that transport and chemistry in this period are represented adequately by the model. Nevertheless, some discrepancies occur, associated with a tendency of the model to overestimate downward tracer fluxes in stratospheric intrusions as also indicated by previous studies. The fact that shallow convection is a sub-grid scale process in the model also hampers a realistic representation of occasional concentration peaks encountered at approximately 2–3 km.

On average, the simulated tropospheric ozone column in summer over the eastern Mediterranean region is about 50 DU. Of this, ~12 DU (25%) is associated with chemically aged and well mixed air, representing typical mid-latitude summer background ozone levels of 15-20 ppbv. The contribution of ozone from stratospheric origin is about 14 DU (30%), and that from lightning emissions is about 6 DU (13%). Contributions from emissions from Europe, SE Asia and North America are 6.8, 3.5 and 3.8 DU,

ACPD
3, 1247–1272, 2003

respectively (together 29%).

Acknowledgement. The work by BS was funded by COACh (Co-operation on Oceanic, Atmospheric and Climate Changes studies, a cooperation between the German and Dutch Ministries for Science and Education). G. J. Roelofs thanks the Dutch computer center SARA (Amsterdam) for use of computer resources.

References

Barry, R. G. and Chorley, R. J.: Atmosphere, weather and climate, Methuen & Co. Ltd., London, UK, 274–328, 1987.

Brühl, C. and Crutzen, P.: Scenarios of possible changes in atmospheric temperature and ozone concentrations due to man's activities, estimated with a one dimensional coupled photochemical climate model, Clim. Dyn., 2, 173–203, 1988.

De Gouw, J., Warneke, C., Holzinger, R., Klüpfel, T., and Williams, J.: Inter-comparison between airborne measurements of methanol, acetonitrile and acetone using two differently configured PTR-MS instruments, Atmos. Chem. Phys., 2003.

Ganzeveld, L. N., Lelieveld, J., and Roelofs, G. J.: A dry deposition parameterization for sulfur oxides in a chemistry-general circulation model, J. Geophys. Res., 103, 5679–5694, 1998.

Heland, J, Ziereis, H., Schlager, H., de Reus, M., Traub, M., and Roelofs, G. J.: Aircraft measurements of nitrogen oxides, ozone, and carbon monoxide during MINOS 2001: distributions and correlation analyses, Atmos. Chem. Phys., 2003.

Jeuken, A., Siegmund, P. C., Heijboer, L. C., Feichter, J., and Bengtsson, L.: On the potential of assimilating meteorological analyses in a global climate model for the purpose of model validation, J. Geophys. Res., 101, 16939–16950, 1996.

Kentarchos, A. S., Roelofs, G. J., and Lelieveld, J.: Altitude distribution of tropospheric ozone over the northern hemisphere during 1996, simulated with a chemistry-general circulation model at two different horizontal resolutions, J. Geophys. Res., 106, 17453–17470, 2001.

Kentarchos, A. S. and Roelofs, G. J.: A model study of stratospheric ozone in the troposphere and its contribution to tropospheric OH formation, J. Geophys. Res., in press, 2003.

Kouvarakis, G., Tsigaridis, K., Kanakidou, M., and Mihalopoulos, N.: Temporal variations of surface regional background ozone over Crete Island in the South-East Mediterranean, J. Geophys. Res., 105, 4399–4407, 2000.

Lawrence, M. G., Rasch, P. J., von Kuhlmann, R., Williams, J., Fisher, H., de Reus, M., Lelieveld, J., Crutzen, P. C., Schultz, M., Stier, P., Huntrieser, H., Heland, J., Stohl, A., Forster, C., Elbern, H., Jakobs, H., and Dickerson, R. R.: Global chemical weather forecasts for field campaign planning: predictions and observations of large-scale features during MINOS, CONTRACE, and INDOEX, Atmos. Chem. Phys. Discuss., 2, 1545–1597, 2002.

Lelieveld, J. and Dentener, F.: What controls tropospheric ozone?, J. Geophys. Res., 105, 3531—3551, 2000.

Lelieveld, J., Berresheim, H., Borrmann, S., Crutzen, P. J., Dentener, F. J., Fischer, H., Feichter, J., Flatau, P. J., Heland, J., Holzinger, R., Kormann, R., Lawrence, M. B., Levin, Z., Markowicz, K., Mihalopoulos, N., Minikin, A., Ramanthan, V., de Reus, M., Roelofs, G. J., Scheeren, H. A., Sciare, J., Schlager, H., Schulz, M., Siegmund, P., Steil, B., Stephanou, E. G., Stier, P., Traub, M., Warneke, C., Williams, J., and Ziereis, H. : Global air pollution crossroads over the Mediterranean, Science, 298, 794–799, 2002.

Meloen, J. Siegmund, P., van Velthoven, P., Kelder, H., Sprenger, M., Wernli, H., Kentarchos, A., Roelofs, G., Feichter, J., Land, C., Forster, C., James, P., Stohl, A., Collins, W., and Cristofanelli, P.: Stratosphere-troposphere exchange: a model and method intercomparison, J. Geophys. Res., in press, 2003.

Millan, M. M., Salvador, R., and Mantilla, E.: Photooxidant dynamics in the Mediterranean basin in summer: results from European research projects, J. Geophys. Res., 102, 8811–8823, 1997.

Rasch, P. J. and Williamson, D.: Computational aspects of moisture transport in global models of the atmosphere, Q. J. R. Meteorol. Soc., 116, 1071–1090, 1990.

Roeckner, E., Arpe, K., Bengtsson, L., Christoph, M., Claussen, M., Dümenil, L., Esch, M., Giorgetta, M., Schlese, U., and Schulzweida, U.: The atmospheric general circulation model ECHAM4: Model description and simulation of present day climate, Max-Planck Institute for Meteorology, Hamburg, Germany, Rep. 218, 1996.

Roelofs, G. J. and Lelieveld, J.: Distribution and budget of ozone in the troposphere calculated with a chemistry-general circulation model, J. Geophys. Res., 100, 20 983–20 998, 1995.

Roelofs, G. J., Lelieveld, J., and van Dorland, R.: A three-dimensional chemistry-general circulation model simulation of anthropogenically derived ozone in the troposphere and its radiative climate forcing. J. Geophys. Res., 102, 23 389–23 401, 1997.

Roelofs, G. J. and Lelieveld, J.: Tropospheric ozone simulation with a global chemistry-climate model: Influence of higher hydrocarbon chemistry, J. Geophys. Res., 105, 22 697–22 712,

2000a.
Roelofs, G. J. and Lelieveld, J.: Model analysis of STE of ozone and its role in the tropospheric O3 budget, in: Chemistry and Radiation Changes in the Ozone Layer, edited by C. Zerefos (ed.), NATO ASI Series, Kluwer Academic Publishers, Netherlands, 25–43, 2000b.
Roelofs, G. J., Kentarchos, A. S., Trickl, T., Stohl, A., Collins, W. J., Crowther, R. A., Hauglustaine, D., Klonecki, A., Law, K. S., Lawrence, M. G., von Kuhlmann, R., and van Weele, M.: Intercomparison of tropospheric ozone models: ozone transports in a complex tropopause folding event, J. Geophys. Res., submitted, 2003.
Scheeren, B., Lelieveld, J., Williams, J., Roelofs, G. J., Fischer, H., de Reus, M., de Gouw, J., Warneke, C., Holzinger, R., Schlager, H., Klüpfel, T., Bolder, M., van der Veen, C., and Lawrence, M.: The impact of monsoon outflow from South-East Asia in the upper troposphere over the eastern Mediterranean, Atmos. Chem. Phys., 2003.
Sprenger, M. and Wernli, H.: A northern hemispheric climatology of cross-tropopause exchange for the ERA15 time period (1979–1993), J. Geophys. Res., in press, 2003.
Stohl, A. and Trickl, T.: A textbook example of long-range transport: Simultaneous observation of ozone maxima of stratospheric and North American origin in the free troposphere over Europe, J. Geophys. Res., 104, 30 445–30 462, 1999.
Thompson, A. M., Pickering, K. E., McNamara, D. P., Schoeberl, M. R., Hudson, R. D., Kim, J. H., Browell, E. V., Fishman, J., Kirchhoff, V. W. J. H., and Nganga, D.: Where did tropospheric ozone over southern Africa and the tropical Atlantic come from in October 1992? Insights from TOMS, GTE/TRACE-A and SAFARI-92, J. Geophys. Res., 101, 24 251–24 278, 1996.
Traub, M., Fischer, H., de Reus, M., Kormann, R., Heland, J., Ziereis, H., Schlager, H., Holzinger, R., Williams, J., Warneke, C., de Gouw, J., and Lelieveld, J.: Chemical characteristics assigned to trajectory clusters during the MINOS campaign, Atmos. Chem. Phys. Disc., 3, 107–134, 2003.

Table 1. Ozone precursor source regions considered in the sensitivity simulations

Source region	Coordinates[a]
India	1° S–33° N, 63° E–89° E
China	1° S–33° N, 90° E–125° E
North America	27° N–75° N, 150° W-27° W
Western Europe	33° N–75° N, 8° W–15° E
Eastern Europe	33° N–75° N, 15° E–35° E
Africa	33° S–33° N, 18° W–50° E

[a] Sensitivity simulations only refer to land-surface emissions.

ACPD

3, 1247–1272, 2003

Table 2. Contributions from source regions to tropospheric ozone columns during MINOS

Source region	O_3 column (DU)	Contribution to O_3 column (%)
Stratosphere (O_3s)	14.3±3.2	29
India	2.0±0.4	4
China	1.5±0.3	3
North America	3.8±0.6	8
Western Europe	3.0±1.5	6
Eastern Europe	3.8±1.5	8
Africa	1.4±0.3	3
Lightning	6.5±0.7	13
Residual	12.3±1.9	25
Total column	48.5±3.0	

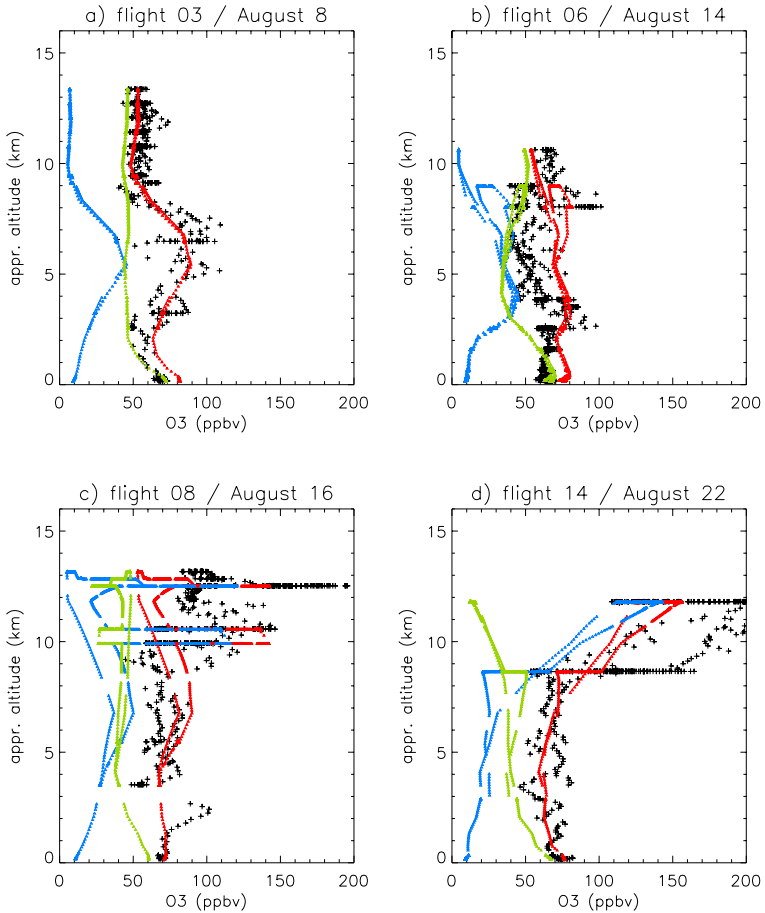

Fig. 1. Vertical profiles of observed ozone (black), modeled ozone (red) and contributions by O_3s (blue) and O_3t (green) for several MINOS flights.

ACPD
3, 1247–1272, 2003

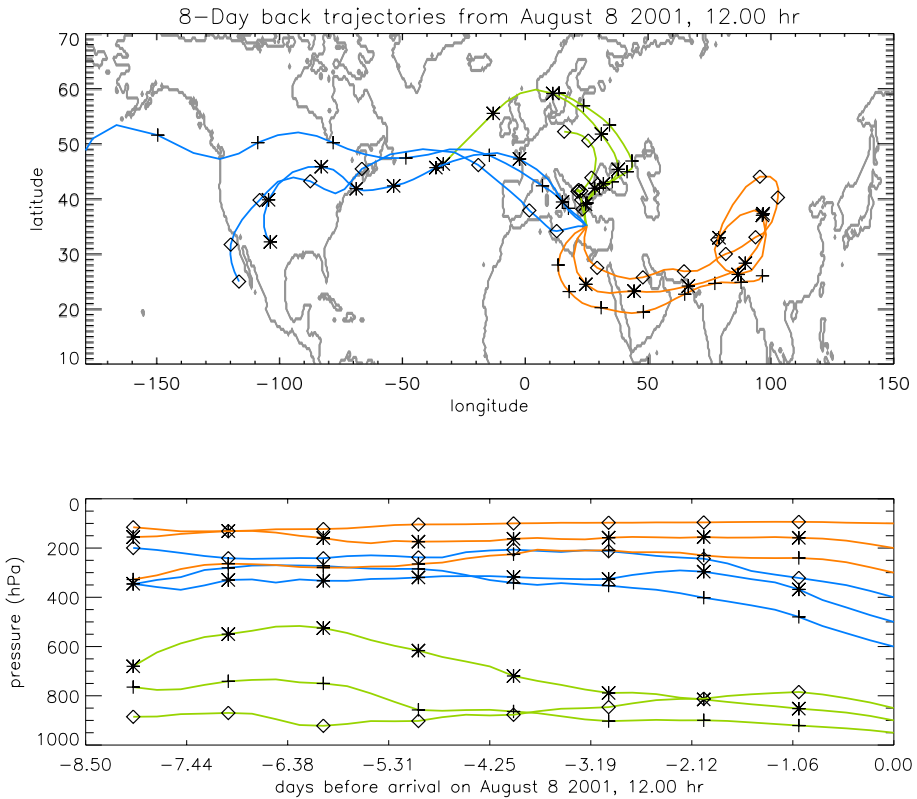

Fig. 2. Eight-day backward trajectories ending at different altitudes above Crete (35° N, 25° E) on 8 August 2001.

ACPD

3, 1247–1272, 2003

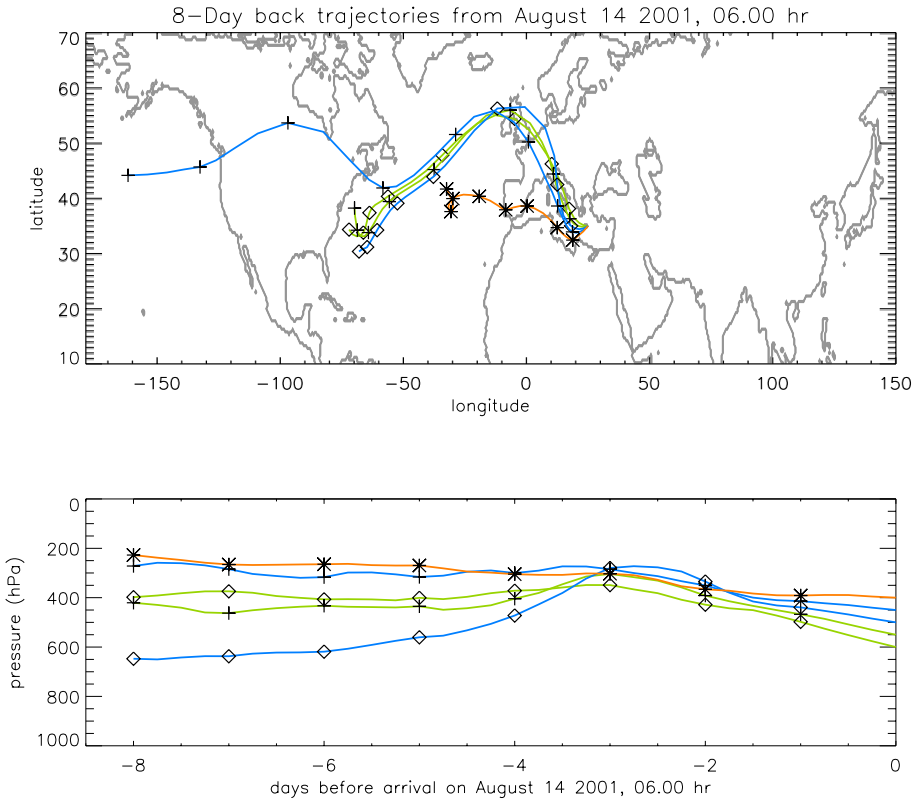

Fig. 3. As Fig. 2 but for 14 August 2001.

ACPD
3, 1247–1272, 2003

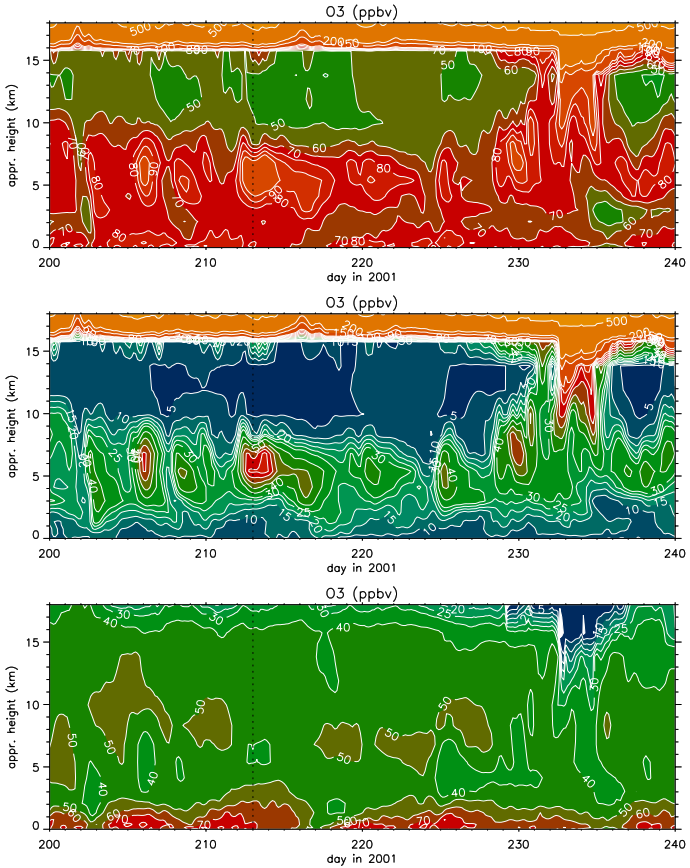

Fig. 4. Simulated time-altitude distributions (ppbv) of **(a)** ozone, **(b)** O_3s, and **(c)** O_3t over Crete (35° N, 25° E) during MINOS. The dotted line refers to 1 August at 00:00 h.

ACPD
3, 1247–1272, 2003

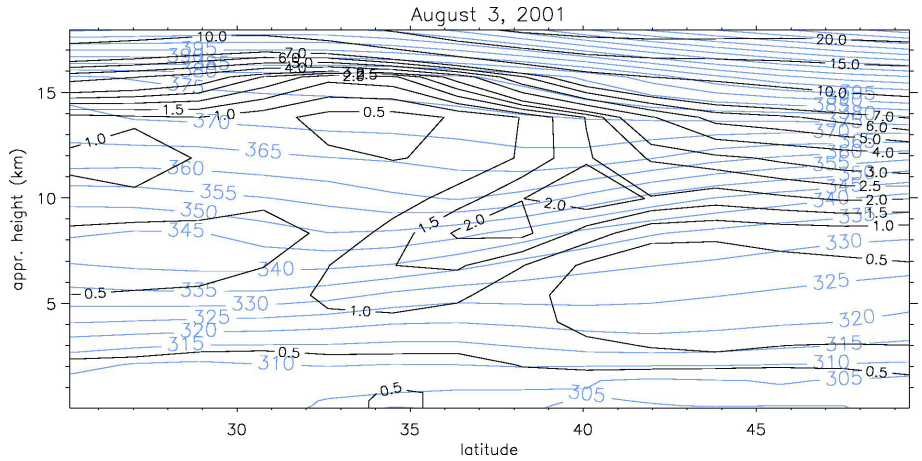

Fig. 5. Simulated time-latitude distributions for 25° E of potential temperature (K, blue) and potential vorticity (PV units, black) for noon time on 3 August 2001.

ACPD

3, 1247–1272, 2003

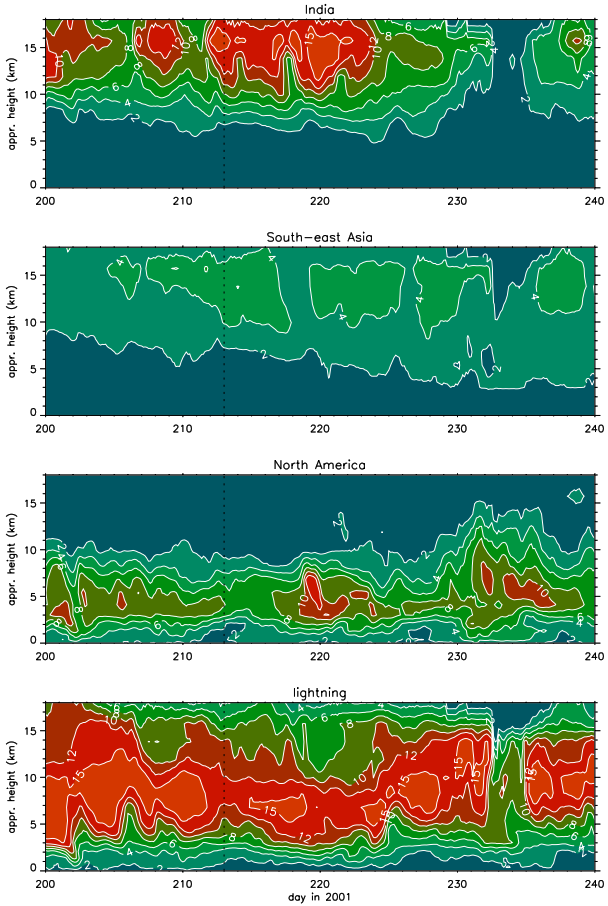

Fig. 6. Simulated time-altitude distributions (ppbv) of photochemically produced ozone due to emissions from **(a)** India, **(b)** China, **(c)** North America, **(d)** lightning (to be continued on the next page).

ACPD
3, 1247–1272, 2003

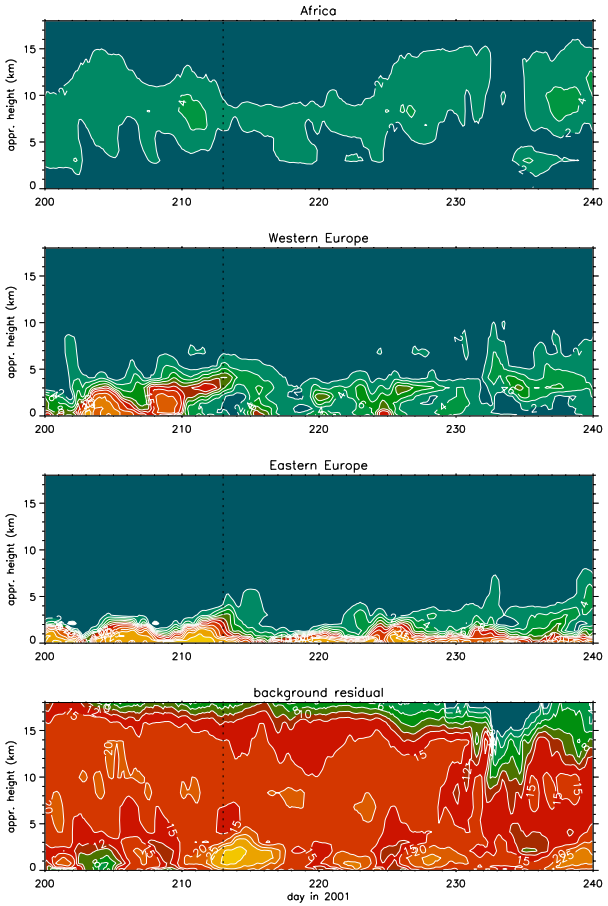

Fig. 6. Continued. **(e)** Africa, **(f)** western Europe, **(g)** eastern Europe, and **(h)** background residual. The dotted line refers to 1 August at 00:00 h.

ACPD
3, 1247–1272, 2003